

PAPER • OPEN ACCESS

Application of a self-compensation mechanism to a rotary-laser scanning measurement system

To cite this article: Siyang Guo *et al* 2017 *Meas. Sci. Technol.* **28** 115007

View the [article online](#) for updates and enhancements.

You may also like

- [Monitoring of lateral displacements of a slope using a series of special fibre Bragg grating-based in-place inclinometers](#)
Hua-Fu Pei, Jian-Hua Yin, Hong-Hu Zhu et al.
- [An innovative geotechnical and structural monitoring system based on the use of NSHT](#)
L Di Gennaro, E Damiano, M De Cristofaro et al.
- [Vehicle platform attitude estimation method based on adaptive Kalman filter and sliding window least squares](#)
Jun Luo, Yongkun Fan, Ping Jiang et al.

Application of a self-compensation mechanism to a rotary-laser scanning measurement system

Siyang Guo , Jiarui Lin , Yongjie Ren, Shendong Shi and Jigui Zhu

State Key Laboratory of Precision Measuring Technology and Instruments, Tianjin University, Tianjin 300072, People's Republic of China

E-mail: linjr@tju.edu.cn

Received 25 April 2017, revised 17 August 2017

Accepted for publication 21 August 2017

Published 17 October 2017



Abstract

In harsh environmental conditions, the relative orientations of transmitters of rotary-laser scanning measuring systems are easily influenced by low-frequency vibrations or creep deformation of the support structure. A self-compensation method that counters this problem is presented. This method is based on an improved workshop Measurement Positioning System (wMPS) with inclinometer-combined transmitters. A calibration method for the spatial rotation between the transmitter and inclinometer with an auxiliary horizontal reference frame is presented. It is shown that the calibration accuracy can be improved by a mechanical adjustment using a special bubble level. The orientation-compensation algorithm of the transmitters is described in detail. The feasibility of this compensation mechanism is validated by Monte Carlo simulations and experiments. The mechanism mainly provides a two-degrees-of-freedom attitude compensation.

Keywords: rotary-laser scanning measuring system, self-compensation, inclinometer, wMPS

(Some figures may appear in colour only in the online journal)

1. Introduction

Distributed measurement systems, especially rotary-laser scanning measuring systems, have shown great potential in the manufacturing industry for meeting ever more demanding requirements for ever larger products (for example, in the shipbuilding industry) [1–3]. The rotary-laser scanning measuring system, with a network of transmitters working cooperatively, has advantages of scalability, concurrent measurement capability, and so on. This system, as with the workshop Measurement Positioning System (wMPS), has been widely applied in the manufacturing industry for tasks such as robot positioning and airplane level measurement [4, 5].

During measurement, multiple transmitters in a rotary-laser scanning measuring system are deployed around the

space and form a spatial measurement network. The stability of the network topology (namely the relative orientation and position of transmitters) is the key element for reliable measurements. In principle, no change in network topology is crucial because it guarantees the same common reference to all the measurement results [6]. With measurement conditions becoming more and more complicated, the distributed nature of such systems causes wMPS to be easily affected by uncontrollable effects which change the topological structure. Small changes in spatial positions induce measurement error which is magnified over distance and leads to non-reliable measurements.

There have been a few solutions developed to keep topological structures stable. The traditional way is to recalibrate the measurement network periodically using the control points and scale bar methods [7]; however, these calibration methods are implemented manually by human operators and repeated calibrations are time consuming and of low efficiency. Yang *et al* present a self-monitoring mechanism by introducing



Original content from this work may be used under the terms of the [Creative Commons Attribution 3.0 licence](https://creativecommons.org/licenses/by/3.0/). Any further distribution of this work must maintain attribution to the author(s) and the title of the work, journal citation and DOI.

redundant receivers [8]. Despite this method being efficient and automatic, it is difficult to keep all receivers stable at all times in a complex environment.

In this paper, an improved rotary-laser scanning measuring system with an inclinometer-combined transmitter is proposed. According to the transmitter's mechanical structure, a two-axis digital inclinometer is fixed onto the transmitter, and mathematical models of the transmitter and inclinometer are introduced. Based on these models, a calibration method for the spatial rotation of the inclinometer with respect to the transmitter is presented with an auxiliary horizontal reference frame. This reference frame, containing more than six target points, is established using an automatic level and laser tracker. Meanwhile, a precise mechanical adjustment with a special bubble level called 'optical composite image level' is carried out to improve the accuracy of calibration. With the built-in inclinometer and calibrated rotation relationship, the relative orientation parameters of transmitters are compensated based on the gravity datum using a related algorithm. This improved system achieves online self-compensation of orientation parameters, which is always influenced by low-frequency vibration (less than 5 Hz, namely the bandwidth of the inclinometer) or long-time creep deformation of the support structure. The online compensation mechanism is a guarantee of the measurement network's stability and accuracy.

This paper is organized as follows: section 2 gives a description of this improved measuring system and the online compensation mechanism. In section 3, related mathematical models are established and the calibration method is elaborated for the transmitter and inclinometer. The compensation algorithm for the orientation parameters is introduced in section 4. In section 5, Monte Carlo simulations are used to evaluate the accuracy of the calibration method. Experiments are prepared in section 6 to prove the validity of this proposed compensation mechanism. Finally, concluding remarks and potential future improvements are provided.

2. Description of the improved rotary-laser scanning measuring system

The improved rotary-laser scanning measuring system is based on a wMPS [9] designed by Tianjin University, China; it consists of rotary-laser transmitters, receivers, and a calculation engine. The transmitters generate signals both from the laser modules in the rotating head and pulsed lasers around the stationary base. Receivers collect such signals and pass them to the calculation engine. The calculation engine converts these signals into angle information and calculates the spatial coordinates of all receivers.

In contrast with the traditional wMPS, this improved system uses a newly developed inclinometer-combined transmitter instead. As shown in figure 1(a), an encoder is installed on the rotating shaft to regulate the rotational speed. The rotating shaft of the transmitter is defined as the z axis. To measure the tilt of the z axis without disturbance from the stationary base, a two-axis digital inclinometer is hung under the encoder on a mechanical structure. The encoder and inclinometer form

a rigid screwed connection. The inclinometer communicates with other devices by WiFi.

The coordinate system of the transmitter is established and defined as $O_t - x_t y_t z_t$. In this coordinate system, the optical axis of one laser module in the rotating head is defined as the x axis. Based on the right-hand rule, the y axis is determined. The coordinate system of the inclinometer is defined as $O_i - x_i y_i z_i$ which uses gravity to lock the z axis. The measurement axes of the inclinometer are defined as the x and y axes, respectively. The intersection point of the measurement axes is defined as the origin of the inclinometer coordinate system.

Figure 1(b) shows how the online compensation mechanism works. The improved wMPS needs network calibration before measurement. Each transmitter of this improved system continuously detects the readings of the built-in inclinometer, and the system estimates the degree of attitude change of each transmitter. If the readings of the inclinometer remain almost the same, it means that the transmitter is not influenced by environmental factors and the measurement network is reliable. If the readings of the inclinometer vary slightly, it means that the transmitter's attitude changes. In this case, the orientation parameters can be automatically compensated by the mechanism. Worst of all is when the readings of the inclinometer show significant differences from the readings before; this compensation mechanism cannot ensure the measurement accuracy. Therefore, this newly developed system will report a warning that recalibration is needed.

3. Calibration method

A precise calibration with a horizontal reference frame is carried out to obtain the relationship between the inclinometer and transmitter coordinate systems.

In this system, three Cartesian coordinate systems are defined: the transmitter coordinate system $O_t - x_t y_t z_t (C_T)$, the inclinometer coordinate system $O_i - x_i y_i z_i (C_I)$, and the horizontal reference frame $O_h - x_h y_h z_h (C_H)$. The inclinometer only senses the gravity vector along its sensitive axis with no fixed origin, so there is only the rotation between the transmitter and inclinometer coordinate systems, and the rotation matrix from the transmitter to inclinometer coordinate systems is defined as R_T^I . The rotation matrix from the transmitter coordinate system to the horizontal reference frame is defined as R_T^H . The rotation matrix from the horizontal reference frame to the inclinometer coordinate system is defined as R_H^I , and we have

$$C_I = R_T^I \cdot C_T = R_H^I \cdot R_T^H \cdot C_T. \quad (1)$$

The whole calibration process is illustrated in figure 2. An auxiliary horizontal reference frame with more than six target points is established using an automatic level, and the rotation matrix is roughly calculated by space resection. The mechanical adjustment uses the optical composite image level to keep the z axis of the transmitter parallel to the direction of gravity. This provides high-precision constraints on two Euler angles of the rotation matrix R_T^H . The rotation matrix R_H^I is obtained based on the mathematical model of the inclinometer.

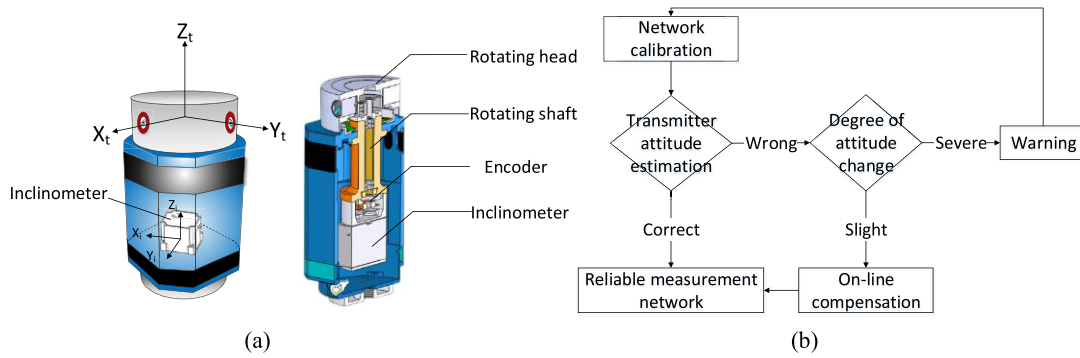


Figure 1. Description of the improved rotary-laser scanning measuring system. (a) Model of inclinometer-combined transmitter and (b) online compensation mechanism.

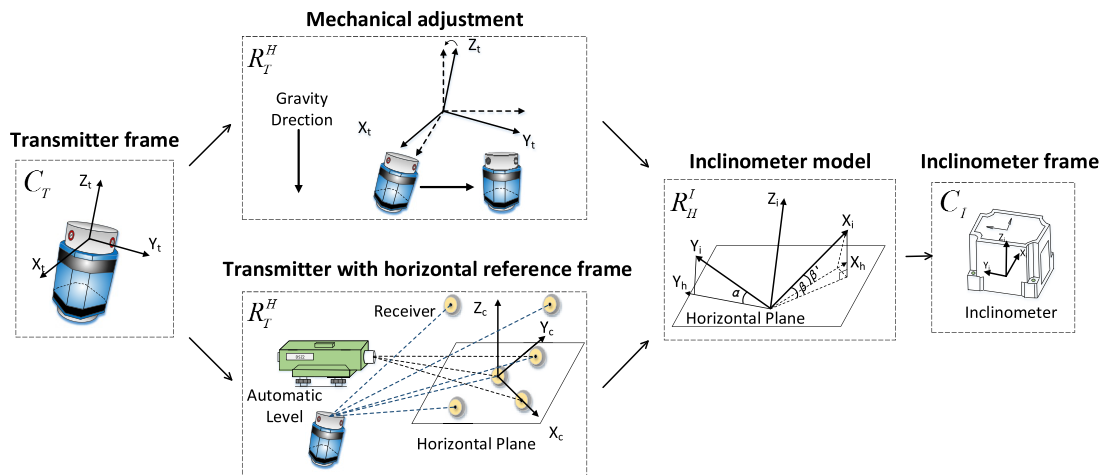


Figure 2. Rotation calibration between transmitter and inclinometer.

According to equation (1), a non-linear optimization method is proposed to obtain the rotation matrix R_T^H .

3.1. Inclinometer measurement model

The geometrical model of a two-axis inclinometer is shown in figure 2. The inclinometer is placed in the space and the output values (α and β) are two inclined angles of the x and y axes of the inclinometer with respect to the horizontal plane. Therefore, there is a rotation (defined as R_H^I) between the inclinometer coordinate system and the horizontal reference frame:

$$R_H^I = R_{y_i} \cdot R_{x_i} \cdot R_{z_i} = \begin{bmatrix} \cos\gamma_i & 0 & \sin\gamma_i \\ 0 & 1 & 0 \\ -\sin\gamma_i & 0 & \cos\gamma_i \end{bmatrix} \begin{bmatrix} 1 & 0 & 0 \\ 0 & \cos\theta_i & -\sin\theta_i \\ 0 & \sin\theta_i & \cos\theta_i \end{bmatrix} \begin{bmatrix} \cos\psi_i & -\sin\psi_i & 0 \\ \sin\psi_i & \cos\psi_i & 0 \\ 0 & 0 & 1 \end{bmatrix} \quad (2)$$

where $R_{x_i}, R_{y_i}, R_{z_i}$ is the rotation matrix from the horizontal to the inclinometer reference frame around the three axes, respectively, and $\theta_i, \gamma_i, \psi_i$ represents the rotation angle around the three axes, respectively.

Assuming that the inclinometer first rotates with the x axis and α is the rotation angle around the y axis, then β' is the rotation angle around the x axis. According to the geometrical relationship between them [10], the rotation angle can be expressed as

$$\begin{cases} \theta_i = \alpha \\ \gamma_i = \beta' = -\arcsin\left(\frac{\sin\beta}{\cos\alpha}\right) \end{cases} \quad (3)$$

Thus, there is only one unknown parameter, ψ_i , in the rotation matrix of the inclinometer with respect to the horizontal reference frame.

3.2. Precise mechanical adjustment

Mechanical adjustment is used to regulate the z axis of the transmitter parallel to the direction of gravity using the total station base and optical composite image level. Figure 3 shows the mechanical adjustment process, with geometrical sketches thereon.

As shown in figure 3(a), the transmitter is fixed to a total station base and the optical composite image level is placed on the transmitter. The V-type working face of the optical composite image level fits closely to the upper surface of the rotation head. There is a tubular bubble in this optical composite image level, and the inclination angle of this with respect to the V-type working face changes when the dial is turned. The transmitter is initially placed at random so that neither the upper surface of the head nor the tubular bubble are parallel to the horizontal direction; because of the installation error, the rotation axis of the transmitter is not perpendicular to the upper surface of the rotation head.

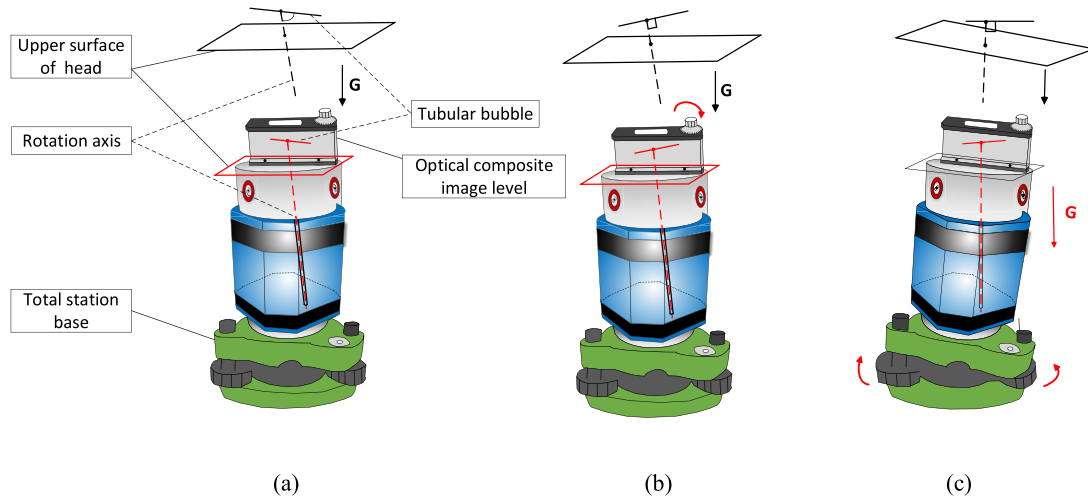


Figure 3. Mechanical adjustment process. (a) Transmitter on the total station base, (b) regulating the optical composite image level and (c) regulating the total station base.

As illustrated in figure 3(b), there is some inclination angle between the tubular bubble and the rotation axis of the transmitter. Turning the dial of this level and rotating the transmitter head 180°, we then observe the bubble in the level. If the bubble remains in a symmetrical position after rotation through 180°, we stop turning the dial; this means that the tubular bubble is perpendicular to the rotation axis.

As illustrated in figure 3(c), the leveling screws of the total station base are turned until the tubular bubble of the level meter is parallel to the horizontal plane. From the lens of optical composite image level, the image of the bubble (which is divided into two parts) is shown: if the tubular bubble is horizontal, the bubble in the tubular bubble moves to the center and the two parts of bubble image coincide. Until now, the tubular bubble has been parallel to the horizontal plane and the rotation axis is parallel to the direction of gravity.

After mechanical adjustment, the z axis of the transmitter is parallel to the direction of gravity, and so a relative rotation relationship between the adjusted transmitter and horizontal reference frame is defined as $(R_T^H)_{\text{calibrated}}$:

$$(R_T^H)_{\text{calibrated}} = R_{yt} \cdot R_{xt} \cdot R_{zt} = \begin{bmatrix} \cos\gamma_t & 0 & -\sin\gamma_t \\ 0 & 1 & 0 \\ \sin\gamma_t & 0 & \cos\gamma_t \end{bmatrix} \begin{bmatrix} 1 & 0 & 0 \\ 0 & \cos\theta_t & \sin\theta_t \\ 0 & -\sin\theta_t & \cos\theta_t \end{bmatrix} \begin{bmatrix} \cos\psi_t & \sin\psi_t & 0 \\ -\sin\psi_t & \cos\psi_t & 0 \\ 0 & 0 & 1 \end{bmatrix} \quad (4)$$

where R_{xt} , R_{yt} , R_{zt} are the rotation matrices around three axes, respectively, and θ_t , γ_t , ψ_t represent the rotation angles around the three axes, respectively.

Based on equations (1), (2), and (4), it can be found that:

$$(R_T^H)_{\text{calibrated}} = k \begin{bmatrix} \cos\psi & -\sin\psi & 0 \\ \sin\psi & \cos\psi & 0 \\ 0 & 0 & 1 \end{bmatrix} \quad (5)$$

$$\text{where } k = \begin{bmatrix} 1 & 0 & 0 \\ 0 & \cos\theta_{ca} & -\sin\theta_{ca} \\ 0 & \sin\theta_{ca} & \cos\theta_{ca} \end{bmatrix} \begin{bmatrix} \cos\gamma_{ca} & 0 & \sin\gamma_{ca} \\ 0 & 1 & 0 \\ -\sin\gamma_{ca} & 0 & \cos\gamma_{ca} \end{bmatrix}$$

θ_{ca} and γ_{ca} are the rotation angles around the x and y axes, respectively, as obtained from the inclinometer when the transmitter has just been regulated and $\psi = \psi_t + \psi_i$.

After mechanical adjustment, the rotation between transmitter and inclinometer has only one unknown value ψ .

3.3. Transmitter with horizontal reference frame

At first, a precise horizontal reference frame C_H is established with an automatic level. The automatic level and magnetic nests are placed in the space. These magnetic nests are the holders for a 1.5 inch diameter sphere on which to place the spherically mounted retroreflector (SMR) of the laser tracker and receiver of this wMPS. More than three magnetic nests are fixed on the vertical guide rail and some others are placed around the space. Each magnetic nest forms a target point. We put the SMR on the magnetic nests which are fixed onto the vertical guide rail and adjust the guide rail to ensure that the center of each SMR is in the same horizontal plane using the automatic level.

Then, the coordinates of each target point are measured by the laser tracker, which is at least one order of magnitude more accurate than the wMPS. The XOY plane of the horizontal reference frame is based on the points in the same horizontal plane with the least-squares surface fitting method. Any point in the XOY plane can be the origin of the horizontal reference frame. Then, a horizontal reference frame C_H is established and the coordinates of the horizontal frame C_H with all the target points are defined as (x_h, y_h, z_h) .

Putting the receiver on these target points of the horizontal reference frame, the relationship [9] between the transmitter and receivers is as follows:

$$\begin{bmatrix} a_m \cos\theta_m + b_m \sin\theta_m \\ a_m \sin\theta_m - b_m \cos\theta_m \\ c_m \\ d_m \end{bmatrix}^T \cdot \begin{bmatrix} R_T^H & T_T^H \\ 0 & 1 \end{bmatrix} \cdot \begin{bmatrix} x_h \\ y_h \\ z_h \\ 1 \end{bmatrix} = 0 \quad (6)$$

where (a_m, b_m, c_m, d_m) are the planar structure parameters of the transmitter, $m = 1, 2$ is the number of planar equations of each transmitter, and θ is the scanning angle around the z axis of the transmitter plane.

Based on equation (6) and the space-resection method [11], R_T^H and T_T^H are obtained.

3.4. Combined solution with weighted nonlinear optimization

The rotation matrix R_H^T and R_T^I can be parameterized as follows:

$$R_H^T = (R_T^H)^{-1} = \begin{bmatrix} r_1 & r_2 & r_3 \\ r_4 & r_5 & r_6 \\ r_7 & r_8 & r_9 \end{bmatrix}, R_T^I = \begin{bmatrix} r_{i1} & r_{i2} & r_{i3} \\ r_{i4} & r_{i5} & r_{i6} \\ r_{i7} & r_{i8} & r_{i9} \end{bmatrix}, \quad (7)$$

where $r_1 \cdots r_9$ are the known values obtained from the space-resection method, and $r_{i1} \cdots r_{i9}$ are to be measured.

Combining equations (1) with (7), we can get

$$R_H^I = R_T^I \cdot R_H^T \Rightarrow \begin{bmatrix} r_{i1}r_1 + r_{i2}r_4 + r_{i3}r_7 & r_{i1}r_2 + r_{i2}r_5 + r_{i3}r_8 & r_{i1}r_3 + r_{i2}r_6 + r_{i3}r_9 \\ r_{i4}r_1 + r_{i5}r_4 + r_{i6}r_7 & r_{i4}r_2 + r_{i5}r_5 + r_{i6}r_8 & r_{i4}r_3 + r_{i5}r_6 + r_{i6}r_9 \\ r_{i7}r_1 + r_{i8}r_4 + r_{i9}r_7 & r_{i7}r_2 + r_{i8}r_5 + r_{i9}r_8 & r_{i7}r_3 + r_{i8}r_6 + r_{i9}r_9 \end{bmatrix} \\ = \begin{bmatrix} \cos\gamma_i \cos\psi_i - \sin\theta_i \sin\gamma_i \sin\psi_i & \sin\theta_i \sin\gamma_i \cos\psi_i + \cos\gamma_i \sin\psi_i & -\cos\theta_i \sin\gamma_i \\ -\cos\theta_i \sin\psi_i & \cos\theta_i \cos\psi_i & \sin\theta_i \\ \sin\theta_i \cos\gamma_i \sin\psi_i + \cos\psi_i \sin\gamma_i & \sin\psi_i \sin\gamma_i - \sin\theta_i \cos\gamma_i \cos\psi_i & \cos\theta_i \cos\gamma_i \end{bmatrix}. \quad (8)$$

By selecting the third column, equation (8) can be rewritten as

$$\begin{cases} r_{i1}r_3 + r_{i2}r_6 + r_{i3}r_9 = -\cos\theta_i \sin\gamma_i \\ r_{i4}r_3 + r_{i5}r_6 + r_{i6}r_9 = \sin\theta_i \\ r_{i7}r_3 + r_{i8}r_6 + r_{i9}r_9 = \cos\theta_i \cos\gamma_i \end{cases}. \quad (9)$$

We put the transmitters with at least three different attitudes by the total station base, and $r_{i1} \cdots r_{i9}$ can be solved by a series of linear equations (see equation (9)). The solution is sensitive to the error introduced by space resection, so a non-linear optimization with the constraints of mechanical adjustment is proposed.

From equation (9), the constraint equations can be written as

$$\begin{cases} F_{n1} = r_{i1}r_{n3} + r_{i2}r_{n6} + r_{i3}r_{n9} + \sin\gamma_{ni} \cos\theta_{ni} \\ F_{n2} = r_{i4}r_{n3} + r_{i5}r_{n6} + r_{i6}r_{n9} - \sin\theta_{ni} \\ F_{n3} = r_{i7}r_{n3} + r_{i8}r_{n6} + r_{i9}r_{n9} - \cos\theta_{ni} \cos\gamma_{ni} \end{cases}. \quad (10)$$

For different transmitter attitudes during calibration, the rotation angles of the inclinometer in the n th attitude of the transmitter are γ_{ni} and θ_{ni} .

The rotation matrix R_H^T satisfies the unit orthogonal constraint conditions

$$\begin{cases} f_1 = r_{i1}^2 + r_{i2}^2 + r_{i3}^2 - 1 = 0 \\ f_2 = r_{i4}^2 + r_{i5}^2 + r_{i6}^2 - 1 = 0 \\ f_3 = r_{i7}^2 + r_{i8}^2 + r_{i9}^2 - 1 = 0 \\ f_4 = r_{i1}r_{i4} + r_{i2}r_{i5} + r_{i3}r_{i6} = 0 \\ f_5 = r_{i1}r_{i7} + r_{i2}r_{i8} + r_{i3}r_{i9} = 0 \\ f_6 = r_{i4}r_{i7} + r_{i5}r_{i8} + r_{i6}r_{i9} = 0 \end{cases}. \quad (11)$$

The mechanical adjustment constraints can be written as follows:

$$\begin{cases} h_1 = \arcsin(r_{i6}) - \theta_{ca} = 0 \\ h_2 = \arctan\left(-\frac{r_{i3}}{r_{i9}}\right) - \gamma_{ca} = 0 \end{cases}. \quad (12)$$

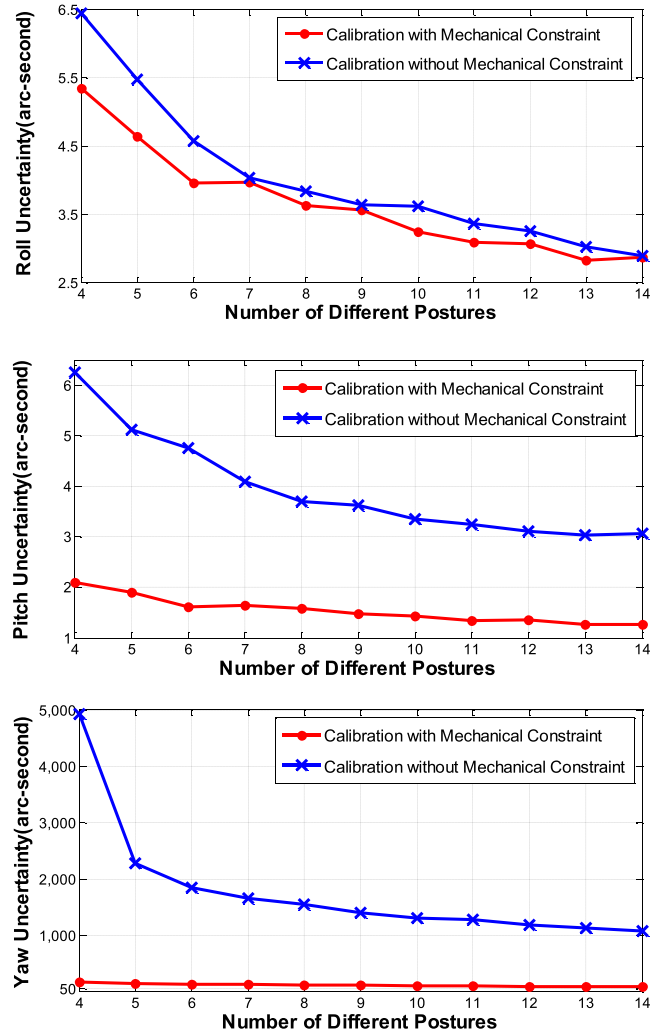


Figure 4. Simulation of calibration method.

From equations (10)–(12), the rotation matrix from the horizontal reference frame to the transmitter coordinate system can be optimized by use of the following functions:

$$E = \sum_{j=1}^n (F_{j1}^2 + F_{j2}^2 + F_{j3}^2) + M \sum_{j=1}^6 f_j^2 + N \sum_{j=1}^3 h_j^2 \quad (13)$$

where M and N are penalty factors. These functions are solved by the Levenberg–Marquardt algorithm [12]. The initial iteration value of the non-linear functions uses the linear solution to equation (9).

4. Orientation parameter compensation algorithm

The attitude of the transmitter is compensated according to the attitude change of the inclinometer. The initial transmitter coordinate system and initial inclinometer coordinate system are defined as $(C_T)_{old}$ and $(C_I)_{old}$. The outputs from the inclinometer are α_{old} and β_{old} along the x and y axes, respectively. The initial rotation matrix R_H^I is defined as $(R_H^I)_{old}$. If the transmitter's attitude changes, the new transmitter coordinate system is defined as $(C_T)_{new}$. Meanwhile, the outputs from the inclinometer are α_{new} and β_{new} in the new inclinometer

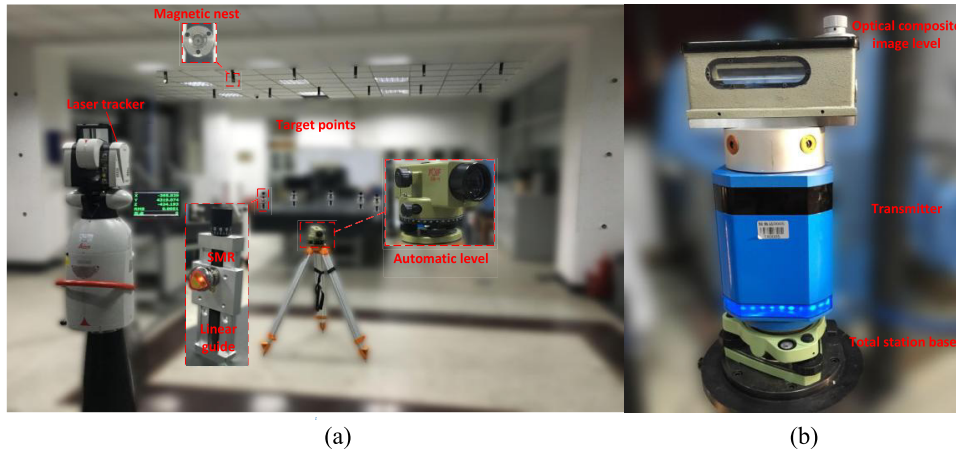


Figure 5. Preparation of rotation calibration: (a) establishment of the horizontal reference frame and (b) mechanical adjustment of the transmitter.

coordinate system $(C_I)_{new}$. The horizontal reference frame remains the same and the rotation matrix R_H^I is defined as $(R_H^I)_{new}$. There are a series of equations used to describe the attitude change of the transmitter:

$$\begin{cases} (R_H^I)_{new} \cdot C_H = (C_I)_{new} \\ (R_H^I)_{old} \cdot C_H = (C_I)_{old} \\ R_T^I \cdot (C_T)_{new} = (C_I)_{new} \\ R_T^I \cdot (C_T)_{old} = (C_I)_{old} \end{cases} \quad (14)$$

where C_H is the horizontal reference frame and R_T^I is the rotation matrix from the transmitter coordinate system to the inclinometer coordinate system. Thus, the new transmitter coordinate system is calculated as follows:

$$(C_T)_{new} = (R_T^I)^{-1} \cdot (R_H^I)_{new} \cdot ((R_H^I)_{old})^{-1} \cdot R_T^I \cdot (C_T)_{old} \quad (15)$$

5. Simulation and analysis

The accuracy of orientation parameter compensation is related to the rotation calibration of the transmitter coordinate system with respect to the inclinometer coordinate system directly. To analyze the accuracy of this calibration method, the Monte Carlo simulation is introduced, combined with related theoretical analysis.

In this simulation, the rotation matrix of the transmitter coordinate system with respect to the inclinometer coordinate system is parameterized by three Euler angles. Roll represents the rotation angle around the x axis, pitch represents the rotation angle around the y axis, and yaw represents the rotation angle around the z axis. This simulation makes a contrast in the uncertainty of the Euler angles, which are calculated by the method with mechanical and without mechanical adjustment, respectively. As mentioned previously, at least three different postures of the transmitter can calculate the rotation matrix. Thus, in the calibration of this simulation, the number of different transmitter postures changes from four to fourteen.

As shown in figure 2, there are three parts of the calibration method and the errors in each part of the calibration are introduced as follows:

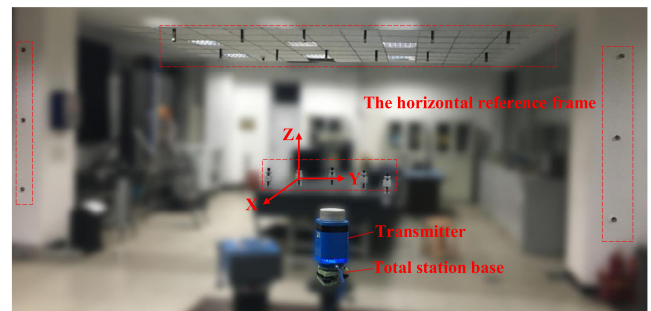


Figure 6. Verification platform of compensation mechanism.

- Rotation calibration of R_T^H with mechanical adjustment: within the range of $\pm 1 \text{ mm m}^{-1}$, the measuring uncertainty of the optical composite image level is 0.01 mm m^{-1} . This ensures that the rotation angle θ_{ca} and rotation angle γ_{ca} of R_T^I have an uncertainty of $2''$.
- Rotation calibration of R_T^H with the space-resection method: the angle measurement accuracy of the transmitter is $2.6''$ (based on three standard deviations) [13]. The horizontal reference frame is established with the automatic level and the laser tracker. For this laser tracker, the maximum permissible error (MPE) of its angular accuracy is $\pm 15 \mu\text{m} + 6 \mu\text{m m}^{-1}$, and the MPE of interferometer accuracy is $\pm 0.4 \mu\text{m} + 0.3 \mu\text{m m}^{-1}$. For the automatic level, which is made in the Suzhou First Optical Instrument Factory, its settling uncertainty is $0.3''$. The standard deviation over a 1 km double run is less than $\pm 1 \text{ mm}$.
- Rotation calibration of R_H^I : the nominal uncertainty of the two-axis inclinometer is $2''$ in each axis.

The results of the simulations are shown in figure 4. As the number of transmitter postures increases, the three Euler angles' uncertainties are decreased. This is because more postures without gross error results in more redundant terms, which increases the accuracy of the solution in the least-square problem. The inclinometer provides just two degrees of freedom in its rotational constraints without the yaw angle, so the yaw uncertainty is larger than the roll and pitch uncertainty. Simulation results also show that all of these three Euler

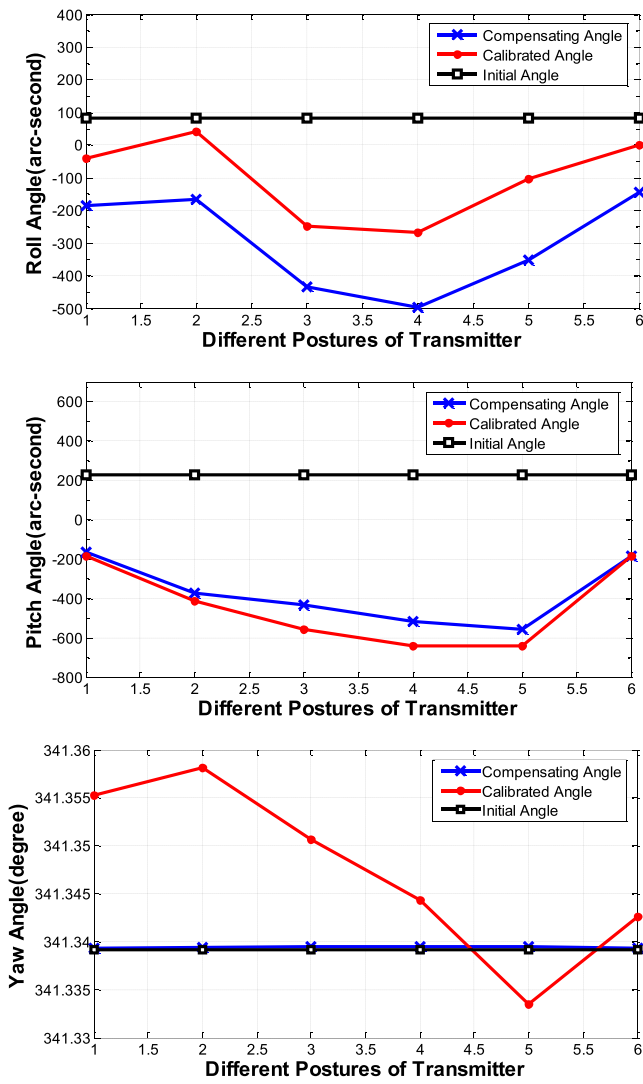


Figure 7. Results of compensating experiments.

angles' uncertainties (after mechanical adjustment) are less than those without mechanical adjustment. This proves that the calibration with mechanical adjustment provides a more accurate rotation matrix than calibration without mechanical adjustment.

6. Experiments

6.1. Establishment of verification platform

The experiment is based on a special transmitter. The inclinometer is installed in the transmitter. Considering the limited space available in the transmitter and its high stability, a dual-axis inclinometer based on a flexible quartz accelerometer is chosen. Its volume is 54 mm × 44.5 mm × 34 mm and has efficient temperature drift compensation and good linearity.

The rotation calibration is shown in figures 5(a) and (b). Figure 5(a) shows the establishment of the horizontal reference frame. Multiple target points with magnetic nests are placed around the space and some special points on the linear guide are adjusted with the help of an automatic level. All the points are measured by the laser tracker as a reference. Figure 5(b) shows the mechanical adjustment of the transmitter with the

optical composite image level and a total station base. With this mechanical adjustment and horizontal reference frame, the rotation matrix of the transmitter with respect to the inclinometer is calibrated.

6.2. Verification of compensation mechanism

With this calibrated rotation matrix of the transmitter coordinate system with respect to the inclinometer coordinate system, the verification experiment is conducted. As shown in figure 6, the transmitter is fixed in place and the rotation matrix of the transmitter coordinate system with respect to the horizontal reference frame is obtained by use of the space-resection method. These three Euler angles of the rotation matrix are named after the initial angle (in black in figure 7). Then, we change the transmitter's posture using the total station base and repeat this test several times. In each set of transmitter postures, three Euler angles of the rotation matrix of the transmitter coordinate system with respect to the horizontal reference frame are obtained using the space-resection method as the reference value, and these angles are shown as a calibrated angle in red in figure 7. In the meantime, three Euler angles which are compensated by the inclinometer form the compensating angles shown in blue in figure 7.

As shown in figure 7, the roll angles of the compensating and calibrated methods have the same tendency. The deviation of the roll angle between these two methods is about 100 to 200 arc-seconds. The pitch angle of the compensating and calibrated methods has the same tendency with ever less deviation. As for the yaw angle, the compensating angle is almost the same as the initial angle. These results prove that the attitude compensation of the roll and pitch angle is valid. Because the inclinometer has just two degrees of freedom in its constraints, the yaw angle is not compensated.

Compared with the simulations, there are more errors introduced to the system in the experiments, such as the error in the internal parameters of the transmitter and the measuring error in the receiver. Also, the Euler angles, which are the reference angles obtained by space resection, contain errors.

7. Conclusions

This article presents an orientation parameter compensation mechanism for a rotary-laser scanning measuring system. This method uses an inclinometer which is fixed in the transmitter to detect attitude change. With mechanical adjustment and the space-resection method, the rotation of the transmitter with respect to the inclinometer is calibrated. Then, the transmitter's attitude-compensating method is presented. Monte Carlo simulations and verification experiments are then carried out. The simulations demonstrate that the calibration of the rotation with mechanical adjustment is more accurate than calibration without mechanical adjustment. After attitude compensation by inclinometer in these experiments, the uncertainty in the roll and pitch angles is less than 200 arc-seconds. The yaw angle is not compensated. The proposed compensation mechanism of the roll and pitch angle is deemed valid, and compensation of the yaw angle failed.

With regard to the proposed method, further research into yaw angle compensation and related position compensation of the transmitters is required. In addition, more accurate calibration of both the transmitter and inclinometer is needed.

Acknowledgments

This work was supported by the National Natural Science Foundation of China (Grant Nos.51775380, 51475329), National Key Research and Development Project of China (Grant No. 2017YFF0204802), and Young Elite Scientists Sponsorship Program by CAST (Grant No. 2016QNRC001).

ORCID iDs

Siyang Guo  <https://orcid.org/0000-0002-4564-9060>

Jiarui Lin  <https://orcid.org/0000-0001-9999-9536>

References

- [1] Peggs G N, Maropoulos P G, Hughes E B, Forbes A B, Robson S, Ziebart M and Muralikrishnan B 2009 Recent developments in large-scale dimensional metrology *Proc. Inst. Mech. Eng. B* **223** 571–95
- [2] Schmitt R H 2016 Advances in large-scale metrology—review and future trends *CIRP Ann.* **65** 643–65
- [3] Franceschini F and Maisano D 2014 The evolution of large-scale dimensional metrology from the perspective of scientific articles and patents *Int. J. Adv. Manuf. Technol.* **70** 887–909
- [4] Norman A R, Schönberg A, Gorlach I A and Schmitt R 2013 Validation of IGPS as an external measurement system for cooperative robot positioning *Int. J. Adv. Manuf. Technol.* **64** 427–46
- [5] Xue B, Zhu J, Yang L, Zhao Z and Ye S 2014 The application of the wMPS in airplane level measurement *Opto-Electron. Eng.* **41** 22–6
- [6] Franceschini F, Galetto M, Maisano D, Mastrogiacomo L and Pralio B 2011 *Distributed Large-Scale Dimensional Metrology. New Insights* (London: Springer Science & Business Media)
- [7] Zhao Z, Zhu J, Xue B and Yang L 2014 Optimization for calibration of large-scale optical measurement positioning system by using spherical constraint *J. Opt. Soc. Am. A* **31** 1427–35
- [8] Yang L H, Wang Y, Zhu J G and Yang X Y 2012 Distributed optical sensor network with self-monitoring mechanism for accurate indoor location and coordinate measurement *Appl. Mech. Mater.* **190** 972–6
- [9] Guo S, Ren Y, Huang Z, Chen Y and Hong T 2015 2D position guidance with single-station optical scan-based system *Int. Conf. on Optical Instruments and Technology 2015* 96230F
- [10] Gao Y, Lin J, Yang L and Zhu J 2016 Development and calibration of an accurate 6-degree-of-freedom measurement system with total station *Meas. Sci. Technol.* **27** 125103
- [11] Liu Z, Zhu J, Yang L, Liu H, Wu J and Xue B 2013 A single-station multi-tasking 3D coordinate measurement method for large-scale metrology based on rotary-laser scanning *Meas. Sci. Technol.* **24** 105004
- [12] Moré J J 1978 The Levenberg–Marquardt algorithm: implementation and theory *Numer. Anal.* **630** 105–16
- [13] Xiong Z, Zhu J, Geng L, Ren Y, Yang X and Ye S 2012 Verification of angle measuring uncertainty for workspace measuring and positioning system *Chin. J. Sens. Actuat.* **2** 019